Analysis and optimization of control cam mechanism in a roller-type corn finger planter based on DEM and MBD coupling technology

Tinghao Deng, Wuyun Zhao, Linrong Shi*, Bugong Sun, Tianshan Qi, Hui Li
(*School of Mechanical and Electrical Engineering, Gansu Agricultural University, Lanzhou 730070, China*)

Abstract: The application of plastic mulch in the arid regions of northwest China has demonstrated significant advantages, making roller-type hole sowing on mulch a key agricultural trend. In order to enhance the performance of a roller-type corn finger planter equipped with finger pickups. This study analyzed the motion patterns of corn seeds within the device and investigated the effects of control cam parameters, including pickup section, vibration section, pickup stroke angle, and torsion spring force, on seed-metering performance. Using DEM-MBD coupling technology, single-factor experiments and second-order orthogonal rotational combination simulation experiments were conducted. The optimal parameter is that pickup section stroke angle is 78.98°, vibration section stroke angle is 20.07°, and a normal force is 2.99 N, which was validated through bench tests, achieving a seed-metering qualification rate of 93.86%, a missed seeding rate of 3.19%, and a reseeding rate of 2.95%. These results met the standards and agronomic requirements, demonstrating the effectiveness of the proposed optimization method. It provides a foundation for improving the precision and reliability of roller-type corn seed-metering devices.

Keywords: corn, roller-type corn finger planter, control cam, DEM-MBD, coupling simulation
DOI: 10.25165/j.ijabe.20251801.9322

Citation: Deng T H, Zhao W Y, Shi L R, Sun B G, Qi T S, Li H. Analysis and optimization of control cam mechanism in a roller-type corn finger planter based on DEM and MBD coupling technology. Int J Agric & Biol Eng, 2025; 18(1): 143–153.

1 Introduction

Corn has rapidly become one of the most significant crops in China due to its "grain-feed-economic crop" three structure attributes[1]. In 2023, China's corn production reached 288.84 million tons, an increase of 11.64 million tons from 2022[2]. With the growing demand for high-yield corn cultivation, advancing mechanization throughout the production process is essential for reducing costs and improving efficiency[3]. Precision planting, a key aspect of precision agriculture, relies heavily on the performance of seed-metering devices, which play a critical role in achieving uniform seed distribution and reducing seed waste[4]. Mechanical seed-metering devices, characterized by their simple structure and adaptability to diverse environments, hold a dominant position in mechanized corn production[5]. They can be further categorized into spoon-type, finger clip-type, clamping-type, and telescopic rod-type based on their operational principles[6]. Among them, the finger clip planter is widely recognized for its uniform seed discharge, low seed damage, and structural simplicity, making it essential for precision planting[7].

Received date: 2024-08-26 **Accepted date:** 2025-01-06
Biographies: **Tinghao Deng**, MS candidate, research interest: agricultural mechanization engineering, Email: 1073323120415@st.gsau.edu.cn; **Wuyun Zhao**, PhD, Professor, research interest: crop production equipment project in northern dry zone, Email: zhaowy@gsau.edu.cn; **Bugong Sun**, PhD, Professor, research interest: crop production equipment project in northern dry zone, Email: sunbg@gsau.edu.cn; **Tianshan Qi**, MS candidate, research interest: agricultural mechanization engineering, Email: 1073323120412@st.gsau.edu.cn; **Hui Li**, MS candidate, research interest: agricultural mechanization engineering, Email: 1073323020188@st.gsau.edu.cn
***Corresponding author: Linrong Shi**, PhD, Associate Professor, research interest: key technologies and equipment for precision seeding in northwest cold and arid zone. Mechanical and Electrical Engineering College, Gansu Agricultural University, Lanzhou 730070, China. Tel: +86-18152092689, Email: shilr@gsau.edu.cn.

To improve the qualification rate of precision seeding, scholars at home and abroad have conducted extensive research and optimization on seed-pickup devices[8]. Shi et al.[9] proposed that the inverted hook be used to prevent the movement of maize seeds up and down in cavity seeders, thereby improving seed filling performance. Li et al.[10] designed a spoon-tongue precise point planter for flax based on the physical characteristics of flax seeds and the requirements of planting agronomy, aiming to address the issues of large seed amounts, high variation coefficients of sowing amounts, and uneven sowing. Zhang et al.[11] proposed a method of adding a secondary seed feeding mechanism between the seed-taking plate and the duckbill to replan the seed movement path, reduce the height of the seed dropping point, and improve the seed discharge performance of the dibbler. Zhang et al.[12] designed a swing-clamp type maize precision seed-metering device to address the issues of missed seed-pickup and multiple pickups during the seed extraction process. By analyzing the influence of population height and seed-metering device rotational speed on the population flow velocity, the seed-metering performance curve of the device was obtained. Li et al.[13] designed a shaped seed- pickup device to address the poor seed filling performance of seed-metering devices under high-speed operation. The feasibility of the structural parameters was verified through a combination of simulation and experimental testing. Lu et al.[14] investigated the effects of hole seeder rotational speed and initial seed velocity on the seeding performance of the hole seeder. They described the working principles of the split seeding system and hole seeder and comprehensively analyzed the causes of missed seeding and reseeding phenomena. Despite these advances, research on roller-type finger pickup planters often neglects the influence of the control cam mechanism, a crucial component that governs the motion of the seed-pickup fingers. Key control cam parameters, such as the pickup section, vibration section, and torsion spring force, play a pivotal role in ensuring the precision and stability of

the seeding process. To address this issue, the present study focuses on the parametric design and optimization of the control cam mechanism in roller-type finger pickup planters.

In this study, a mechanical model of the seed-pickup process is developed to analyze the interaction between seed-pickup fingers and corn kernels. Simulation experiments were first conducted to evaluate the effects of individual control cam parameters, including the pickup section stroke angle, vibration section stroke angle, and the normal force exerted by the torsion spring, on the seed-metering performance. These parameters were systematically varied across predefined ranges under constant simulation conditions to establish their individual impacts. Following the single factor simulations, coupling simulations using EDEM and RecurDyn software were employed to perform a second-order orthogonal rotational combination experiment for parameter optimization. The simulation results were further validated through bench tests to confirm the effectiveness of the proposed optimization approach.

2 Material and methods

2.1 Overall structure

As shown in Figure 1, the roller-type corn finger planter comprises two main categories of components: core functional modules and auxiliary components. Core modules include the seed dispensing module (duckbill dibbler and connecting inserts), connecting shaft, platen, end cover, connecting insert, core disc, regulating cam, ejector finger clip clamping module, duckbill hole-former, seed pickup disc, and fixing plate. These components are securely assembled using bolts, forming a compact and efficient mechanism.

2.2 Working principle

The working process consists of five distinct operational zones: seed-taking zone, seed-carrying zone, seed-cleaning zone, primary seed-dispensing zone, and secondary seed-dispensing zone. Seed-taking zone: The seed-pickup fingers open under the drive of the handle and connecting rod, creating a space for corn seeds to enter. Gravity guides the seeds into the seed-pickup space created by the opening seed-pickup fingers. Seed-carrying zone: The pickup fingers disengage from the control cam constraint, and the torsion spring forces the pickup spoon to close, securely clamping the seeds. The fingers then follow a uniform circular motion. Seed-cleaning zone: Any excess seeds clamped by the fingers are brushed off by the brush, which ensures that only one seed remains securely clamped. Primary seed-dispensing zone: The clamped corn seed is ejected toward the duckbill dibbler under the torsion spring force. Secondary seed-dispensing zone: The duckbill dibbler opens, releasing the seed into the soil. The seed is buried, completing the seeding cycle. This process ensures precise seed distribution while minimizing seed waste and mechanical interference. Figure 2 illustrates the workflow, highlighting the sequential operations in each zone.

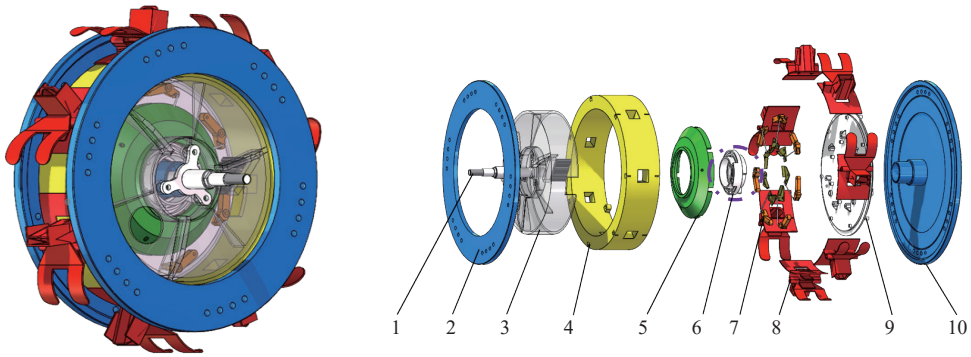

a. Assemble structure b. Component structure

1. Connecting shaft 2. Platen 3. End cover 4. Connecting insert 5. Core disc 6. Regulating cam 7. Ejector finger Clip clamping module 8. Duckbill hole-former 9. Seed pickup disc 10. Fixing plate

Figure 1 Structure of roller-type corn finger planter

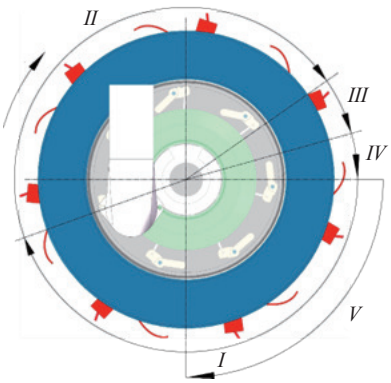

Ⅰ. Seed-taking zone Ⅱ. Seed-carrying zone Ⅲ. Seed-cleaning zone Ⅳ. Primary seed-dispensing zone Ⅴ. Secondary seed-dispensing zone

Figure 2 Zone division of working process of roller-type corn finger planter

2.3 Corn simulation model

Three typical shapes of Zhengdan 958 corn seeds were selected: dent corn, conical corn, and spheroid corn[15]. Fifty seeds of each type (Gansu Longfengxiang Seed Co.) were measured, and the measurements are listed in Table 1. Corn seed models were constructed in EDEM software with spherical particles. The modeling details for each type are as follows: The dent corn seed model consists of nine particles of varying diameters, the spherical conical corn seed model consists of three particles of varying diameters, and the spheroid corn seed model consists of a single spherical particle. The three corn seed models and the dimensions are visually illustrated in Figure 3. A ratio of 5:3:1 for dent corn, conical corn, and spheroid corn seeds was used to generate a total of 1000 seeds for the simulation. The selected parameters ensure the accurate modeling of seed interactions and their behavior during the seeding process. Table 2 summarizes the simulation parameters for both the corn seeds and the dibbler materials used in simulation.

2.4 Coupling model

This study uses DEM-MBD coupling simulation to analyze the cam parameters of the finger pickup-type corn seed-metering device. On the performance of metering seed, EDEM simulates the

flow of corn seeds, while RecurDyn simulates the movement of the seed-metering device. During coupling, the components of the seed-metering device that come into contact with the corn seed models are exported as wall files from RecurDyn. The remaining components are merged, and the wall files are imported into EDEM to establish the coupling model. The simulation determines whether the corn seed models are in contact with the seed-metering device at each step through contact detection. Based on the overlap, the interaction forces between the corn seed models and the seed-metering device are calculated for each time step. These forces are transmitted to both EDEM and RecurDyn, and the program iterates to complete the remaining calculations. The specific simulation steps are as follows: (1) RecurDyn calculates the kinematic parameters (position, velocity, acceleration) and dynamic parameters (constraint forces and torques) of each component of the seed-metering device. (2) EDEM retrieves the position data of the seed-metering device components from RecurDyn. (3) RecurDyn calculates the interaction forces between the corn seed models and the components of the seed-metering device. (4) EDEM starts the iterative calculations for the corn seed models at the current time step. (5) EDEM transmits the forces and torques exerted by the corn seed models on the seed-metering device components back to RecurDyn, and the RecurDyn module updates the kinematic parameters (position, velocity, acceleration) and dynamic parameters (joint constraint forces and driving forces) of the components. This iterative process continues until the specified simulation time is reached, ensuring precise modeling of the interaction between corn seeds and the seed-metering device. Figure 4 illustrates the coupled simulation model, highlighting the real-time exchange of forces and kinematic data between EDEM and RecurDyn.

Table 1 Corn seed dimensions

Item	Dent corn				Conical corn			Spheroid corn
	Length L/mm	Upper width W_1/mm	Lower width W_2/mm	Height T/mm	Length L/mm	Upper width W_1/mm	Lower width W_2/mm	Length L/mm
Maximum value/mm	13.28	1.87	8.96	7.24	12.96	9.74	7.87	10.53
Minimum value/mm	9.35	7.62	5.83	3.18	8.76	6.05	4.92	6.77
Average value/mm	11.60	9.39	7.15	5.07	11.14	8.00	6.27	8.84
Standard deviation	1.18	0.98	1.14	1.12	1.31	1.16	0.89	1.31

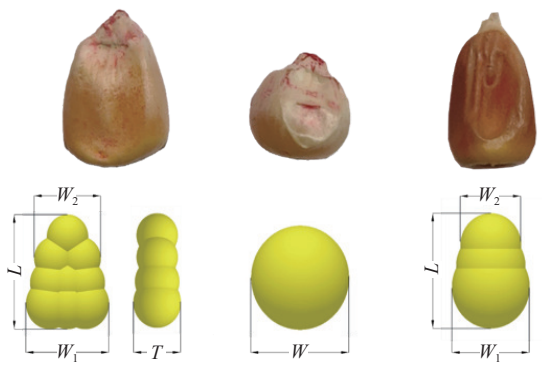

a. Dent corn b. Conicalcorn c. Spheroid corn

Figure 3 Discrete element model of corn seeds

Table 2 Simulation parameters

Parameters	Value
Poisson's ratio of corn seeds	0.4[18]
Shear modulus of corn seeds/Pa	1.37[9]
Density of corn seeds/kg·m^{-3}	1196[21]
Collision recovery coefficient of corn seeds	0.37[20]
Static friction coefficient of corn seeds	0.2[19]
Poisson's ratio of ABS plastic	0.34[16]
Shear modulus of ABS plastic/Pa	2.3[16]
Density of ABS plastic/kg·m^{-3}	1.25[16]
Rolling friction coefficient of dent corn	0.013[9]
Rolling friction coefficient of conical corn	0.024[9]
Rolling friction coefficient of spheroid corn	0.053[9]
Rolling friction coefficient of dent-conical	0.004[9]
Rolling friction coefficient of dent-spheroid	0.003[9]
Rolling friction coefficient of conical-spheroid	0.014[9]
Recovery coefficient of corn-ABS	0.41[17]
Static friction coefficient of corn-ABS	0.462[17]
Rolling friction coefficient of corn-ABS	0.178[17]

3 Results and discussion

3.1 Analysis of the working process of the seed-metering device

3.1.1 Analysis of the seed-pickup process

The seed-picking process is the initial stage of the seed-metering device's operation and is critical for ensuring seeding quality. Proper adjustment of the opening and closing time, as well as the stroke angle of the seed-pickup fingers, significantly improves seed-picking performance. The control cam, shown in Figure 5, plays a pivotal role in regulating the opening and closing motion of the seed-pickup fingers. It consists of four functional segments: the plow segment, vibration segment, picking segment, and seed-carrying segment. The centerline segment *AD* of the control cam comprises three arc segments: *AB*, *BC*, and *CD*. Plow segment (*AB*): Aligns the seed flow for optimal entry into the pickup zone. Vibration segment (*BC*): Introduced to alleviate seed accumulation and improve seed flow consistency during the pickup process. Picking segment (*CD*): Facilitates secure seed picking and clamping by adjusting the cam profile.

During the seed-picking process, the seed-picking fingers are driven by the seed-metering device through a double rocker mechanism. The sequence of operations is as follows: (1) Cam-driven opening: The drive handle contacts the control cam, gradually overcoming the spring tension and causing the seed-picking fingers to open to their maximum capacity. This creates a seed-pickup space where corn seeds, influenced by gravity and inter-seed interactions tore, enter. (2) Seed pickup: The seed-pickup fingers reach the end of the seed picking-zone (point *D*), where the drive handle disengages from the control cam. The increasing spring tension causes the seed-picking fingers to close, securely clamping one or more seeds. (3) Spring-driven clamping: As the seed-pickup fingers move into the seed-carrying segment, spring tension maintains consistent clamping pressure to ensure the corn seeds are securely transported into the seeding segment. During the seed-carrying process, the seed-picking fingers deliver the corn seeds with controlled pressure into the duckbill dibbler. The dibbler then deposits the seeds into the soil, completing the seeding cycle. This sequence ensures smooth and precise seed delivery throughout the entire seeding operation.

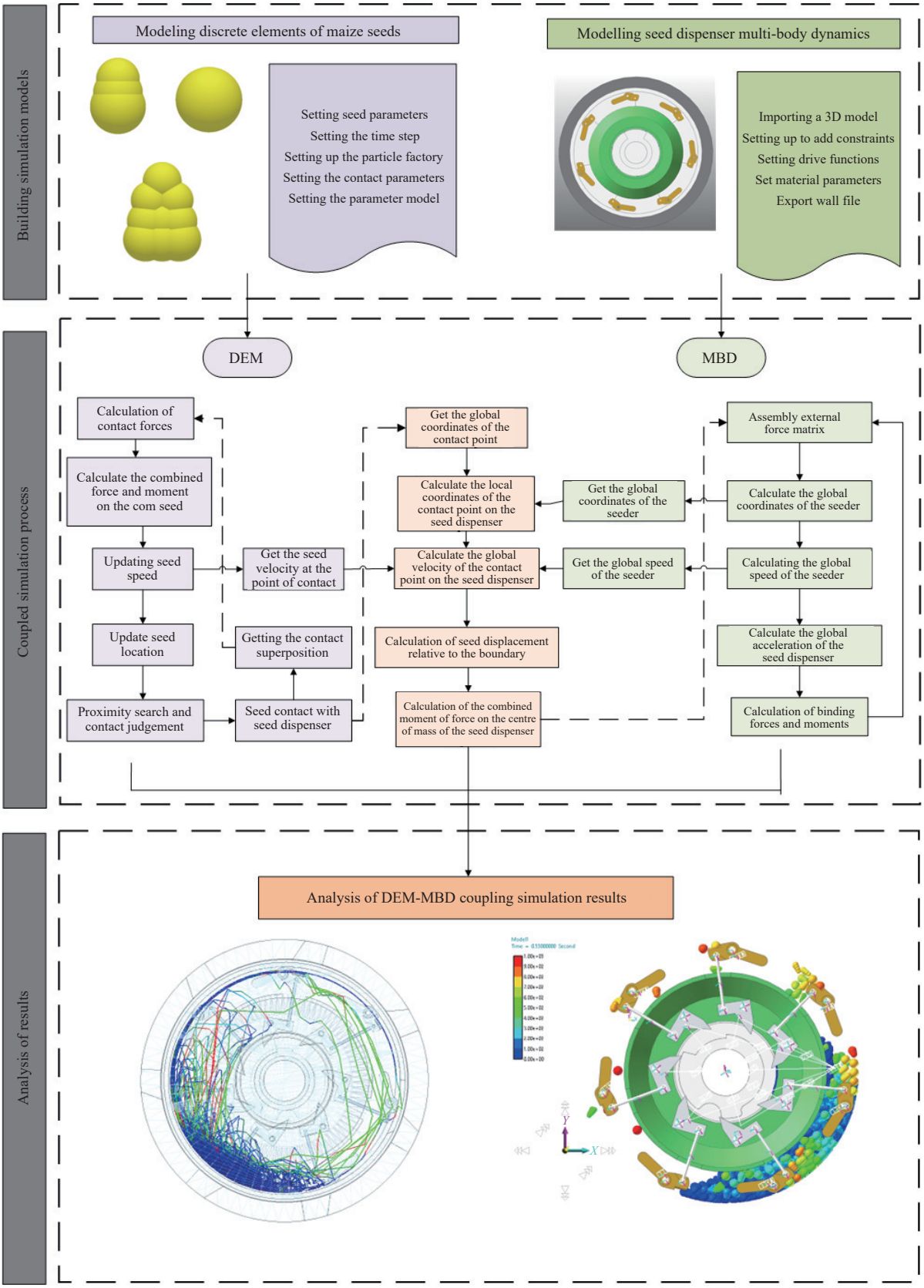

Figure 4 Coupling calculation process

(1) Simulation analysis of the plow segment

The plow segment (*AB*) was critical for the seed-pickup process, defined as an arc with the control cam's rotation center *O* as the center and the distance between the crank end and *O* as the radius. During this stage, the seed-picking fingers rotate clockwise around *O*, driven by the connecting rod and drive handle, to open the seed-picking zone and create the seed-picking space. The stroke angle and posture of the seed-picking fingers during this segment significantly influenced the efficiency of picking seed. The stroke angle of the plow segment determines the opening and closing time of the seed-pickup fingers. A larger stroke angle results in a longer opening and closing time. Previous studies, such as Wang et al.[22], have shown that an optimal charging angle of 85° improves seed-picking performance. This study simulated plow segment stroke

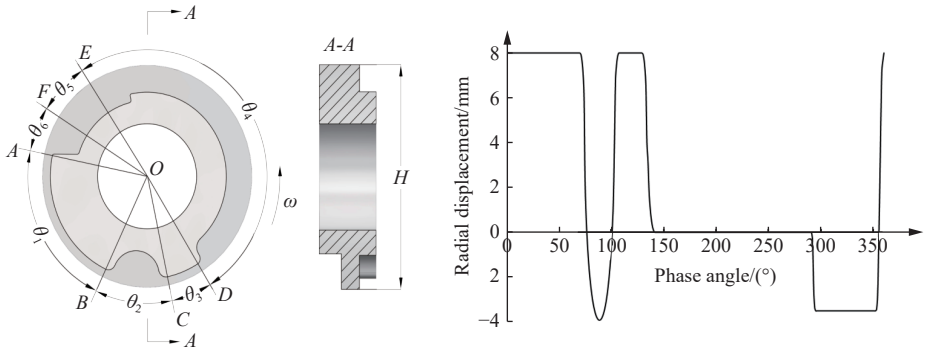

a. Structural diagram b. phase curve

Figure 5 Schematic diagram of the control cam profile

angles of 60°, 70°, 80°, 90°, and 100° to evaluate their effects on the efficiency of picking seed. Using RecurDyn software, simulations were performed at a seed-metering device speed of 25 r/min with a simulation time of 10 s. Each condition was repeated three times. Metering seed performance indices (seed-metering qualification rate, miss seeding rate, and reseeding rate) were calculated according to the GB/T 6979-2005[23] "Test Methods for Precision Seeders". The results are summarized in Table 3.

Table 3 and Figure 6 show that the stroke angle of the plow segment significantly affected the performance of metering seed. At smaller stroke angles of 60°, the seed-picking fingers closed prematurely, limiting their penetration into the corn seed population. This led to a high missed seeding rate, averaging 8.98%, as shown in Figure 7a, due to low seed population pressure. As the stroke angle increased to 80°, the seeding qualification rate reached a maximum average of 95.36%, with a low missed seeding rate of 2.05% and a reseeding rate of 2.59%. This occurred because the seed-pickup fingers achieved stable contact with the corn seed population, ensuring effective pickup. At larger stroke angles of 100°, the extended opening phase delayed the subsequent picking phase. When the seed-pickup fingers closed, they were positioned above the corn seed population with lower pressure, increasing the likelihood of seeds being ejected and resulting in a higher missed seeding rate, averaging 4.73%, as shown in Figure 7b.

Table 3 Simulation results of metering seed effect at different scooping section angles

Stroke angle/(°)	No.	Seed-metering qualification rate/%		Missed seeding rate/%		Reseeding rate/%	
		Value	Average	Value	Average	Value	Average
60	1	91.08	89.15	1.62	1.87	7.30	8.98
	2	87.06		2.05		10.89	
	3	89.31		1.95		8.74	
70	1	90.25	91.43	3.24	3.7	6.51	4.87
	2	90.18		4.12		5.70	
	3	93.86		3.75		2.39	
80	1	96.62	95.36	2.62	2.59	1.81	2.05
	2	98.06		1.83		1.76	
	3	94.40		3.32		2.58	
90	1	94.08	94.82	2.43	2.29	2.72	2.89
	2	96.09		2.91		2.79	
	3	94.39		1.54		3.15	
100	1	93.12	94.08	1.03	1.19	5.85	4.73
	2	95.32		1.25		3.43	
	3	93.80		1.28		4.92	

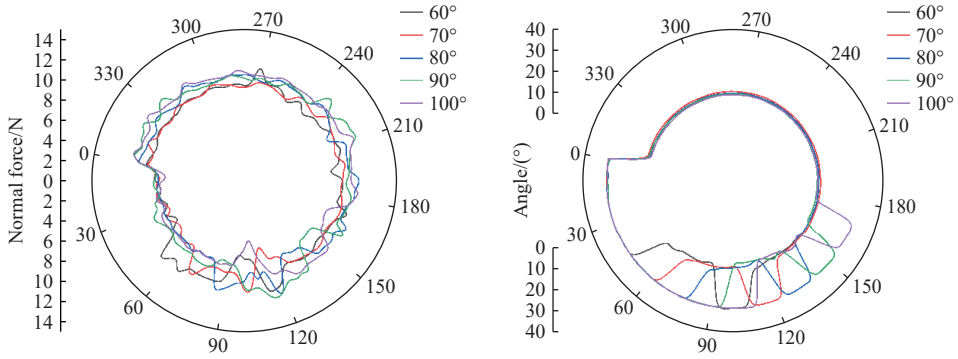

a. Normal force b. Angle

Figure 6 Effect of different plow segment section angles on the normal force and angle of the seed-picking finger

In summary, the plow segment's stroke angle significantly impacts the metering seed quality of the seed-metering device. A stroke angle that is too small causes the seed-pickup fingers to close prematurely, leading to missed seeding due to insufficient seed population contact. Conversely, an excessively large stroke angle reduces seed population pressure during the pickup process, which also results in missed seeding. An optimal stroke angle of 80° achieves the best seeding performance, balancing the seeding qualification rate, reseeding rate, and missed seeding rate.

(2) Simulation analysis of the vibration segment

The vibration segment (*BC*) is an inwardly concave arc with its center located at a point on the crank end, and the radius slightly larger than the drive handle stroke. During this segment, the seed-picking fingers rotate clockwise around the control cam's rotation center *O*, rapidly close and reopen. The primary function of the vibration segment is to disturb the corn seed population, reduce clogging, and ensure that clamped seeds remain secure. To analyze the impact of vibration segment stroke angles on the performance of

picking seed, simulations were conducted at a seed-metering device speed of 25 r/min, consistent with the plow segment simulation. Five vibration segment stroke angles (30°, 35°, 40°, 45°, and 50°) were tested, with each condition repeated three times. Seed-metering qualification rates and reseeding rates at each angle were measured, and the results are listed in Table 4.

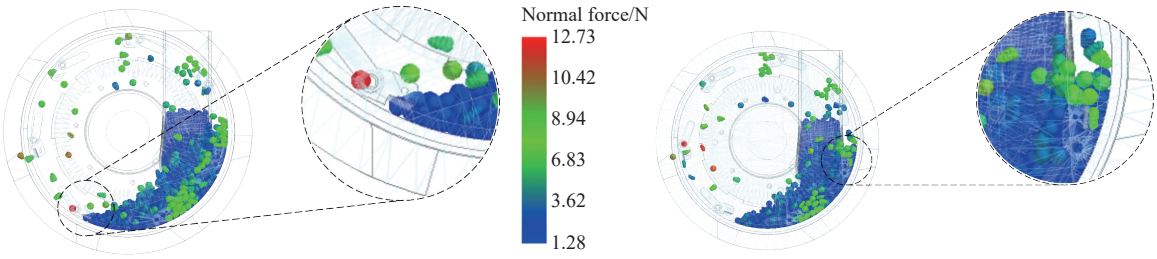

a. 60° b. 100°

Figure 7 Comparison of the seed stress at different plow segment angles push angles

Table 4 Simulation results of the effect of different vibration sections of the thrust angle taking species

Stroke angle/(°)	No.	Shoveling section seed metering qualification rate/%		Vibration section seed metering qualification rate/%		Reseeding rate/%	
		Value	Average	Value	Average	Value	Average
30	1	94.08	95.41	93.99	95.34	2.49	2.70
	2	96.41		96.35		2.86	
	3	95.73		95.68		2.76	
35	1	94.08	94.65	94.03	94.54	2.39	2.64
	2	95.80		95.59		2.85	
	3	94.07		94.01		2.67	
40	1	93.12	94.08	93.09	94.04	1.37	1.47
	2	95.32		95.27		1.46	
	3	93.80		93.77		1.59	
45	1	94.08	94.85	94.03	94.79	1.46	1.51
	2	96.09		96.04		1.48	
	3	94.39		94.30		1.58	
50	1	93.12	94.08	93.11	94.04	1.57	1.50
	2	95.32		95.27		1.49	
	3	93.80		93.75		1.44	

Table 4 indicates that as the vibration segment stroke angle increases, the seed-metering qualification rate remains relatively stable, while the reseeding rate initially decreases and then stabilizes. At smaller stroke angles of 30°, the seed-picking fingers fail to complete their swinging motion, leading to inadequate disturbance of the seed population, as shown in Figure 8a. This results in seed clogging and reduced seeding efficiency. At a stroke angle of 40°, the seed-picking fingers complete their full swinging motion within the vibration segment, effectively disturbing the seed population and minimizing clogging. The reseeding rate reaches its lowest average value of 1.47%, as shown in Table 5 and Figure 8b. However, further increases in the stroke angle to 50° cause the seed-picking fingers to close prematurely after completing the swinging motion. This state does not contribute positively to the seed-picking process and should be avoided, as shown in Figure 8c. Figure 9a shows that the normal force exerted by the seed-picking fingers on the seed population remains consistent across larger stroke angles. When the stroke angle is less than 35°, the normal force decreases significantly, indicating insufficient disturbance of the seed population. At larger stroke angles, the seed-pickup fingers engage effectively with the seed population, ensuring efficient seed disturbance. This ensures that the fingers maintain consistent pressure on the seeds, reducing the reseeding rate while maintaining stability. Furthermore, the extended motion eliminates any seed accumulation or clogging that might occur at smaller stroke angles, thereby improving the overall efficiency and reliability of the seed-metering device, reducing the reseeding rate while maintaining stability. Combined with the stroke angle changes shown in Figure 9b, it can be concluded that a stroke angle of less than 35° fails to provide adequate seed disturbance, leading to seed clogging and reduced performance of metering seed.

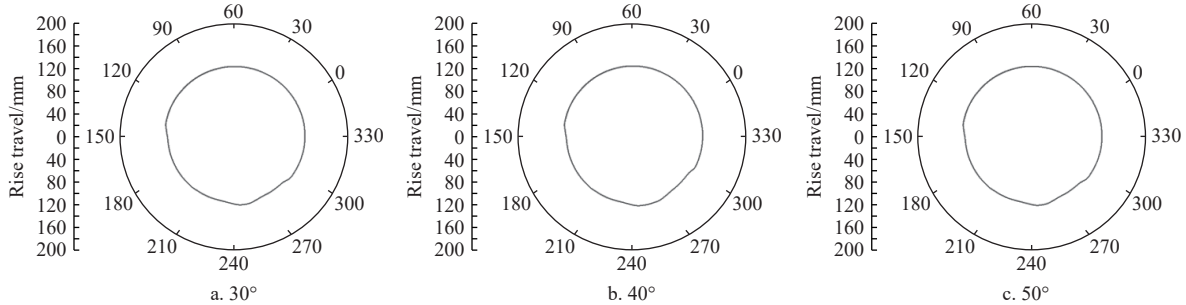

a. 30° b. 40° c. 50°

Figure 8 Swinging trajectory of the seed-picking finger under different vibration segment angles

The vibration segment stroke angle plays a critical role in optimizing seed-picking performance. When the stroke angle is too small, the seed-picking fingers cannot complete the required swinging motion, leading to seed clogging and poor disturbance of the seed population. Conversely, when the stroke angle is too large, the seed-pickup fingers close prematurely after swinging, resulting in increased stroke angles throughout the seed-pickup stage without improvement of metering seed performance. The optimal stroke angle of 40° achieves the best balance, ensuring effective seed disturbance and minimal reseeding rates.

(3) Simulation analysis of the picking segment

The picking segment (*CD*) is an arc centered on the rotation

center O of the control cam, with a radius determined by the distance between the crank end and O. During this stage, the seed-picking fingers rotate clockwise around O, creating and maintaining the seed-pickup space. As the final stage of the seed-picking process, the picking segment aims to extend the seed-pickup time, adjust the posture of the clamped seeds, and ensure that they remain securely held. The seed-picking fingers must maintain an upward orientation throughout this segment to prevent seeds from falling off. To investigate the impact of picking segment stroke angles on performance, simulations were conducted under the same rotation speed and simulation time as the plow and vibration segments. Stroke angles were set to 10°, 15°, 20°, 25°, and 30°, with three repetitions for each condition. Seed-metering qualification rates at each angle were recorded and are summarized in Table 5.

Table 5 shows that the seed-metering qualification rate initially increases with the picking segment stroke angle but decreases after exceeding a certain value. At small stroke angles of 10°-15°, the stroke angle changes minimally as the seed-picking fingers pass through the picking segment, as shown in Figure 10b. However, significant fluctuations in the normal force are observed at the end of this segment, as seen in Figure 10a. These fluctuations improve seed picking in some cases but can cause instability in the seed population, leading to missing seed. Figure 11a illustrates that at a 10° stroke angle, the seed population experiences severe force fluctuations, which are detrimental to seed pickup. At the optimal stroke angle of 20°, the seed-pickup qualification rate reaches its highest average value of 96.53%, as shown in Table 5. At this angle, the normal force stabilizes, as shown in Figure 10a, and the seed-picking fingers maintain consistent contact with the seed population, resulting in improved performance of picking seed. The movement of the seed-picking fingers and the seed population stress conditions are optimized at this angle, as seen in Figure 11b. When the stroke angle is 30°, the seed-picking time becomes excessively long, positioning the seed-picking fingers above the corn seed population by the end of the picking segment, as illustrated in Figure 11d. In this position, the clamped seeds experience reduced normal force, making them prone to ejection when the seed-pickup fingers close. This significantly increases the missed seeding rate.

Table 5 Simulation results of the metering seed effect of different picking section stroke angles

Stroke angle/(°)	Num	Vibration section seed- metering qualification rate/%		Seed-metering qualification rate/%	
		Value	Average	Value	Average
10	1	93.84	94.04	91.83	92.66
	2	94.03		92.86	
	3	94.24		93.28	
15	1	93.95	94.03	94.68	93.87
	2	94.16		93.24	
	3	93.98		93.68	
20	1	93.99	93.99	95.68	96.53
	2	93.86		96.74	
	3	94.11		97.18	
25	1	94.36	94.53	94.36	94.42
	2	94.52		94.25	
	3	94.72		94.64	
30	1	94.51	94.12	94.18	93.35
	2	94.09		92.84	
	3	93.76		93.04	

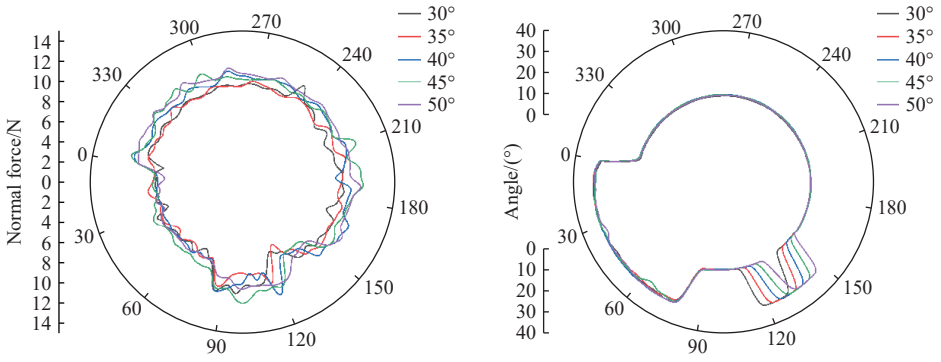

a. Normal force b. Angle

Figure 9 Effect of different vibration segment section angles on the normal force and angle of the seed-picking finger

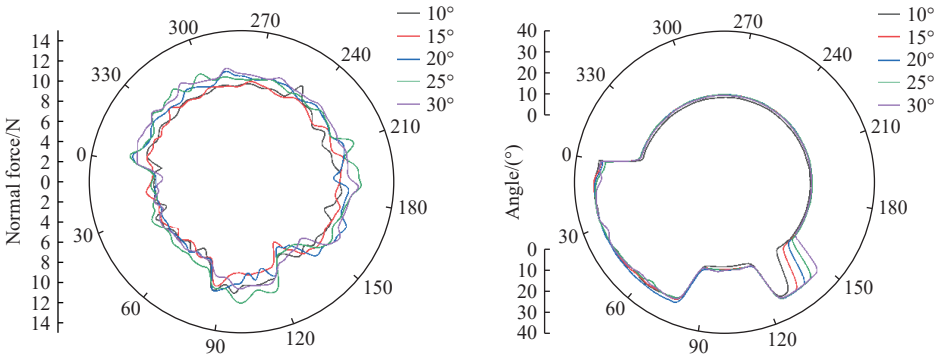

a. Normal force b. Angle

Figure 10 Effect of different picking segment stroke angles on the normal force and angle of the seed- picking finger

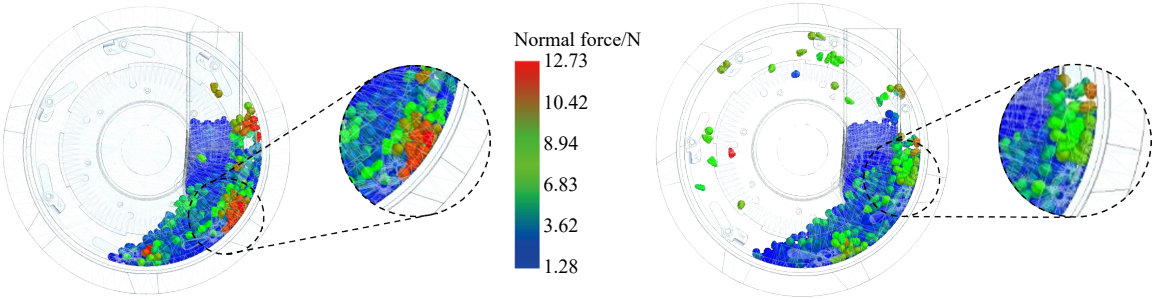

a. 10° b. 30°

Figure 11 Comparison of the seed stress at different picking segment stroke angles

The picking segment stroke angle significantly impacts the seed-pickup qualification rate of the seed-metering device. When the stroke angle is too small, the normal force fluctuates significantly, leading to instability in the seed population and an increased missed seeding rate. When the stroke angle is too large, the seed-pickup fingers close above the corn seed population, failing to securely clamp the seeds, which also results in missing seed. At the optimal stroke angle of 20°, the seed-pickup fingers achieve stable motion and consistent seed clamping, maximizing the seed-metering qualification rate and minimizing missed seeding. Thus, a picking segment stroke angle of 20° is recommended to achieve the best balance between seeding performance and seed-pickup stability.

3.1.2 Analysis of the seed-carrying process

After completing the seed-pickup stage, the drive handle disengages from the control cam, and the spring force gradually closes the seed-picking fingers, securely clamping one or more corn seeds. The torsion spring ensures that the pickup spoon closes securely, holding the seeds in place and preventing dislodgment caused by vibrations or irregular device motion. The spring calibrated tension is critical for balancing the clamping force, securely holding seeds without damaging them, thereby optimizing seeding precision and reliability. Figure 12 illustrates the normal forces experienced by dent, conical, and spheroid corn seeds under varying spring forces during the seed-carrying process.

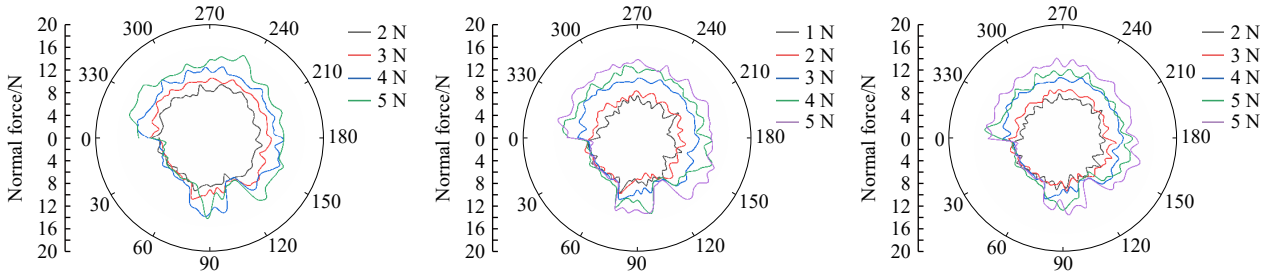

a. Dent corn b. Conical corn c. Spheroid corn

Figure 12 Normal force on corn seeds under different finger clamping forces

As shown in Figure 12a, when the spring force was 2 N, the normal force on the corn seeds varied significantly throughout the seed-carrying process. Observations revealed that the seed-metering qualification rate for dent corn seeds was relatively low under this condition. The thinner shape of dent corn seeds resulted in insufficient opening and closing amplitudes of the seed-pickup fingers, and the transmitted normal force was inadequate to counteract seed weight and inertia, leading to slippage and higher missed seeding rates. Figures 12b and 12c show that conical and spheroid corn seeds experienced more stable normal forces than dent corn seeds. When the spring force increased to 3 N or 4 N, the normal force stabilized across all seed types. At a spring force of 3 N, the stress variations on conical and spheroid corn seeds were minimal, ensuring consistent clamping and improved seed-metering qualification rates.

To address the instability observed at 2 N, increasing the spring force to 3 N significantly reduced normal force variations, ensuring stable clamping and consistent seed-metering qualification rates. However, while 4 N further stabilized seed clamping, it provided limited improvement over 3 N and risked accelerating wear on the seed-picking fingers over time. Therefore, a spring force of 3 N is recommended to achieve the best balance between seed-pickup stability and device efficiency during the seed-carrying stage.

3.2 Second-order rotational orthogonal regression test

3.2.1 Test design

To investigate the effects of the plow segment stroke angle, picking segment stroke angle, and normal force on the seed-pickup fingers, along with their quadratic and interaction terms, on the seeding performance of the roller-type corn seed-metering device, a second-order rotational orthogonal regression combination test was conducted. The speed of the seed-metering device was set to 25 r/min. Table 6 summarizes the encoding of the test factors.

Table 6 Factors and codes

Encodings	Considerations		
	Push angle of plow segment x_1/(°)	Push angle of picking segment x_2/(°)	Seed-pickup pinch normal force x_3/N
–1	70.0	15.0	2.00
0	80.0	20.0	3.00
1	90.0	25.0	4.00

3.2.2 Test results analysis

Based on the test scheme, experimental results were analyzed to evaluate the effects of key factors on the performance of metering seed. The results of the quadratic orthogonal regression test are listed in Table 7. Using Design-Expert 8 software, variance analysis was performed on the seed-metering qualification rate (Y_1), missed

seeding rate (Y_2), and reseeding rate (Y_3). Table 8 presents the analysis of variance, where X_1, X_2, and X_3 represent the plow segment stroke angle, picking segment stroke angle, and normal force on the seed-pickup fingers, respectively.

(1) Seed-metering qualification rate Y_1

From Table 8, it can be seen that the fitting degree of the qualification rate model is p=0.0045, which is extremely significant (p<0.01), and the lack-of-fit term is p=0.3050, which is not significant (p>0.05). This indicates that there are no other main factors affecting the qualification rate, and the Y_1 regression equation does not have a lack of fit. The primary factors affecting the qualification rate of the seed-metering device are the plow segment stroke angle X_1, normal force on the seed-pickup fingers X_3, and picking segment stroke angle X_2. The quadratic terms X_1^2, X_2^2, and X_3^2 have extremely significant effects. After removing the non-significant interaction terms, the regression model equation is:

$$Y_1 = 94.21 - 0.11X_1 + 0.011X_2 - 0.029X_3 - 0.45X_1^2 - 0.28X_2^2 - 0.32X_3^2 \quad (1)$$

(2) Missed seeding rate Y_2

From Table 8, it can be seen that the fitting degree of the missed seeding rate model is p=0.0040, which is extremely significant (p<0.01), and the lack-of-fit term is p=0.5074, which is not significant (p>0.05). This indicates that there are no other main factors affecting the missed seeding rate, and the Y_2 regression equation does not have a lack of fit. The primary factors affecting the missed seeding rate of the seed-metering device are the plow segment stroke angle X_1, normal force on the seed-pickup fingers X_3, and picking segment stroke angle X_2. The terms X_1, X_3, X_1^2, and X_3^2 have extremely significant effects. After removing the non-significant interaction terms, the regression model equation is:

$$Y_2 = 3.42 + 0.23X_1 0.036X_2 + 0.21X_3 + 0.22X_1^2 + 0.21X_3^2 \quad (2)$$

Table 7 Experimental results

Serial number	Considerations			Experimental indicators		
	X_1	X_2	X_3	Y_1/%	Y_2/%	Y_3/%
1	–1	–1	0	93.54	3.52	2.94
2	1	–1	0	93.31	3.94	2.75
3	–1	1	0	93.67	3.34	2.99
4	1	1	0	93.4	3.79	2.81
5	–1	0	–1	93.49	3.46	3.05
6	1	0	–1	93.24	3.92	2.84
7	–1	0	1	93.59	3.76	2.65
8	1	0	1	93.42	4.23	2.35
9	0	–1	–1	93.76	3.33	2.91
10	0	1	–1	93.71	3.42	2.87
11	0	–1	1	93.52	3.92	2.56
12	0	1	1	93.44	3.87	2.69
13	0	0	0	94.05	3.53	2.42
14	0	0	0	94.12	3.27	2.61
15	0	0	0	94.38	3.42	2.20
16	0	0	0	94.31	3.54	2.15
17	0	0	0	94.17	3.32	2.51

Table 8 Analysis of variance

Source	Y_1				Y_2				Y_3			
	Sum of squares	Df	F-value	p-value	Sum of squares	Df	F-value	p-value	Sum of squares	Df	F-value	p-value
Model	1.90	9	8.79	0.0045**	1.17	9	9.14	0.0040**	0.99	9	4.41	0.0316**
X_1	0.11	1	4.40	0.0741	0.41	1	28.47	0.0011**	0.097	1	3.86	0.0901
X_2	0.0010	1	0.042	0.8432	0.011	1	0.74	0.4185	0.005	1	0.20	0.6686
X_3	0.0066	1	0.28	0.6161	0.34	1	23.92	0.0018**	0.25	1	10.06	0.0157*
XX_{12}	0.0004	1	0.017	0.9010	0.0002	1	0.016	0.9035	0.002	1	0.0009	0.9757
XX_{13}	0.0016	1	0.067	0.8038	0.0025	1	0.0017	0.9677	0.002	1	0.081	0.7844
XX_{23}	0.0002	1	0.0093	0.9256	0.0049	1	0.34	0.5757	0.007	1	0.29	0.6079
X_1^2	0.85	1	35.36	0.0006**	0.20	1	14.26	0.0069**	0.22	1	8.87	0.0206*
X_2^2	0.32	1	13.42	0.0080**	0.0006	1	0.043	0.8423	0.30	1	11.78	0.0110*
X_3^2	0.44	1	18.14	0.0038**	0.18	1	12.68	0.0092**	0.055	1	2.21	0.1805
Residual	0.17	7			0.100	7			0.18	7		
Lack of fit	0.094	3	1.69	0.3050	0.041	3	0.92	0.5074	0.019	3	0.16	0.9185
Pure error	0.074	4			0.059	4			0.16	4		
Sum	2.07	16	8.79	0.0045	1.27	16	9.14	0.0040	1.17	16	4.41	0.0316

Note:** indicates highly significant (p<0.01); * indicates significant (0.01≤p<0.05)

(3) Reseeding rate Y_3

From Table 8, it can be seen that the fitting degree of the reseeding rate model is p=0.0316, which is significant (p<0.05), and the lack-of-fit term is p=0.9185, which is not significant (p>0.05). This indicates that there are no other main factors affecting the reseeding rate, and the Y_3 regression equation does not have a lack of fit. The primary factors affecting the reseeding rate of the seed-metering device are the normal force on the seed-pickup fingers X_3, plow segment stroke angle X_1, and picking segment stroke angle X_2. The terms X_3, X_1^2, and X_2^2 have significant effects. After removing the non-significant interaction terms, the regression model can be expressed as:

$$Y_3 = 2.38 - 0.11X_1 + 0.025X_2 - 0.18X_3 + 0.23X_1^2 + 0.26X_2^2 \quad (3)$$

3.2.3 Parameter optimization

To obtain the optimal factor, the boundary conditions of the factors were combined with the regression models of Equations (1)-(3). The goal was to maximize the qualification rate and minimize the missed seeding rate and reseeding rate. Based on the boundary conditions of each factor value, a model for parameter optimization was established. The objective function and constraints were set, and the optimization results showed that the optimal parameter combination is a plow segment stroke angle of 78.98°, a picking segment stroke angle of 20.07°, and a normal force of 2.99 N. Under this parameter combination, the seed-metering qualification rate is 94.21%, the missed seeding rate is 3.39%, and the reseeding rate is 2.39%.

$$\begin{cases} \begin{cases} \max Y_1 \\ \min Y_2 \\ \min Y_3 \end{cases} \\ \text{s.t} \begin{cases} 70^\circ \le x_1 \le 90^\circ \\ 15^\circ \le x_2 \le 25^\circ \\ 2N \le x_3 \le 4N \end{cases} \end{cases} \tag{4}$$

3.3 Bench test

To validate the actual performance of the roller-type corn finger planter, a regulating cam was created based on the optimal parameter combination and installed in the planter. A bench validation test was conducted referencing the standard GB/T 6973-2005 "Test Methods for Precision Seeders", as shown in Figure 13.

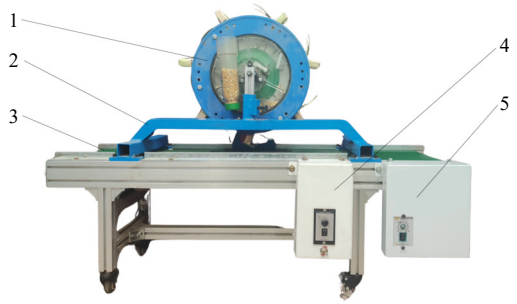

1. Seed rower 2. Frame 3. Conveyor belt 4. Speed control box 5. Transformer

Figure 13 Bench validation test

The test was set with a rotation speed of 25 r/min. After the test bench had operated for a certain period and the seed-metering device was working stably, data recording began. Each group recorded 300 sets, and the test was repeated three times to obtain average values. The qualification rate, missed seeding rate, and reseeding rate were calculated, with the test results shown in Table 9. According to Table 9, under the optimal parameter combination, the seed-metering device achieved a seed-metering qualification rate of 93.86%, missed seeding rate of 2.95%, and reseeding rate of 3.19%. Differences in results are attributed to variations in material properties and environmental factors, such as friction coefficients, seed moisture content, and external disturbances during bench tests. While simulations assume ideal conditions, real-world tests involve uncontrollable variables, leading to minor discrepancies. However, overall trends in qualification rates, missed seeding rates, and reseeding rates showed strong alignment between simulations and experimental outcomes, validating the proposed optimization parameters. This result confirms that the operating performance under the optimal parameter combination meets the requirements for the roller-type corn seed-metering device with finger pickup.

Table 9 Test validation results

No.	Seed-metering qualification rate/%	Missed seeding rate/%	Reseeding rate/%
1	94.36	2.81	2.83
2	93.14	3.81	3.05
3	94.08	2.96	2.96
Average	93.86	3.19	2.95

4 Conclusions

(1) This study utilized DEM-MBD coupling technology to simulate the working process of a roller-type corn seed-metering device with finger pickups and investigated the effects of control cam parameters on seeding performance. The results demonstrated that the stroke angles in the plow, vibration, and picking segments, as well as the normal force on the seed-pickup fingers, significantly influence seeding quality. Specifically, improper stroke angles in different segments can result in issues such as missed seeding, seed accumulation, or seed clogging, while inappropriate normal forces during the seed-carrying stage may lead to seed loss or damage. The findings highlight the importance of precise control of these parameters in ensuring optimal performance.

(2) The study established an optimal parameter combination for the plow segment stroke angle of 78.98°, the picking segment stroke angle of 20.07°, and the normal force of 2.99 N, achieving a seed-metering qualification rate of 94.21%, a missed seeding rate of 3.39%, and a reseeding rate of 2.39%. Bench test results were consistent with simulation outcomes, validating the proposed optimization approach and demonstrating its reliability. These findings provide valuable insights for improving the precision and efficiency of seed-metering devices, contributing to advancements in precision agriculture technology.

(3) Future work will explore the adaptability of the proposed optimization method for other crops with diverse seed shapes and sizes. Additionally, investigating the long-term durability and field performance of the optimized device under varying environmental conditions will further validate its applicability and expand its use in precision agriculture systems.

Acknowledgements

The authors acknowledge that this work was financially supported by the Fuxi Young Talent Cultivation Project of Gansu Agricultural University (Grant No. gaufx-05y02), National Natural Science Foundation of China (Grant No. 52365030), and The Science and Technology Innovation Fund of Gansu Agricultural University-Young Mentor Support Fund Project (Grant No. GAU-QDFC-2024-06)

[References]

[1] Liu Q W, Cui T, Zhang D X, Yang L, Wang Y X, He X T, et al. Design and experimental study of seed precise delivery mechanism for high-speed maize planter. Int J Agric & Biol Eng, 2018; 11(4): 81–87.

[2] National statistical office. Announcement by the national statistical office on grain production data for 2023. 2023. Available: https://www.gov.cn/lianbo/bumen/202312/content_6919545.htm. Accessed on [2024-04-25].

[3] Huang Z F, Xue J, Ming B, Wang K R, Xie R Z, Hou P, et al. Analysis of factors affecting the impurity rate of mechanically-harvested maize grain in China. Int J Agric & Biol Eng, 2020; 13(5): 17–22.

[4] Li Y H, Yang L, Zhang D X, Cui T, Zhang K L, Xie C J, et al. Analysis and test of linear seeding process of Corn high speed precision metering device with air suction. Transactions of the CSAE, 2020; 36(9): 26–35. (in Chinese)

[5] Dong J X, Zhang S L, Zheng Z Z, Wu H T, Huang Y X, Gao X J Development of a novel perforated type precision metering device for efficient and cleaner production of maize. Journal of Cleaner Production, 2024; 443: 140928.

[6] Yang L, Yan B X, Zhang D X, Zhang T L, Wang Y X, Cui T. Research progress on precision planting technology of corn. Transactions of the CSAM, 2016; 47(11): 38–48. (in Chinese)

[7] Wang J W, Tang H, Wang J F, Shen H G, Feng X, Wang H N. Analysis and experiment of guiding and dropping migratory mechanism on pickup dropping migratory mechanism on pickup. Transactions of the CSAM, 2017; 48(1): 29–37,46. (in Chinese)

[8] Dai F, Zhao Y M, Liu Y X, Shi R J, Xin S L, Fu Q F, et al. Analysis and performance test on dynamic seed corn threshing and conveying process with variable diameter and spacing. Int J Agric & Biol Eng, 2023; 16(2): 259–266.

[9] Shi L R, Zhao W Y, Hua C T, Rao G, Wang Z. Study on the intercropping mechanism and seeding improvement of the cavity planter with vertical insertion using DEM-MBD coupling method. Agriculture, 2022; 12: 1567.

[10] Li H, Zhao W Y, Shi L R, Dai F, Rao G, Wang Z. Design and test of seed ladle tongue type flax precision burrow planter. Transactions of the CSAM, 2024; 55(3): 85–95. (in Chinese)

[11] Zhang C Y, Kang J M, Peng Q J, Zhang N N, Wang X Y, Jian S C. Design and test of secondary seed feeding mechanism of air-suction roller dibbler for cotton. Transactions of the CSAM, 2021; 52(6): 106–116. (in Chinese)

[12] Zhang X J, Cheng J P, Shi Z L, Wang J M, Fu H, Wu H F. Simulation and experiment of seed taking performance of swing-clamp type corn precision seed-metering device. Transactions of the CSAM, 2023; 54(4): 38–50. (in Chinese)

[13] Li C, Cui T, Zhang D X, Yang L, He X T, Jing M S, et al. Design shaped hole inserts by simulating and analysing the high-speed filling posture of maize seed particles. ScienceDirect, 2023; 232: 29–50.

[14] Lu B, Ni X D, Li K Z, Li S F, Qi Q Z, Shao W P. Simulation analysis and experiment of seed discharge performance of high-speed hole seeder based on EDEM. Journal of Chinese Agricultural Mechanization, 2024; 45(2): 49–54. (in Chinese) DOI: 10.13733/j.jcam.issn.2095 5553.2024.02.008

[15] Shi L R, Zhao W Y, Rao G, Wang Z. Modeling of typically shaped corn seeds and calibration of the coefficient of rolling friction. Agronomy, 2023; 13: 1573.

[16] Takayama T. vickers hardness mechanical models and thermoplastic polymer injection-molded products' static friction coefficients. Manufacturing and Materials Processing, 2024; 8(1): 11;

[17] Shi L R, Zhao W Y, Sun W, Yang X P, Wang G P, Xin S L. Analysis of the metering performance for typical shapemaize seeds using DEM. Int J Agric & Biol Eng, 2023; 16(1): 26–35.

[18] Horabik J, Molenda M. Parameters and contact models for DEM simulations of agricultural granular materials. Biosystems Engineering, 2016; 147: 206–225.

[19] Wang L J, Zhou W X, Ding Z J, Li X X, Zhang C G. Experimental determination of parameter effects on the coefficient of restitution of differently shaped corn in three-dimensions. Powder Technol, 2015; 284: 187–194.

[20] Markauskas D, Ramírez-Gómez Á, Kačianauskas R, Zdancevičius E. Corn grain shape approaches for DEM modelling. Compute. Electron. Agric., 2015; 118: 247–258.

[21] Sun Y H, Guo J H, Shi L R. Design and parameter optimization of air-suction wheel type of seed-metering device with elastic pad for maize. Int J Agric & Biol Eng, 2024; 17(4): 116–127.

[22] Wang J W, Tang H, Guan R, Li X, Bai H C, Tian L Q. Optimization design and experiment on clamping static and dynamic finger-spoon maize precision seed metering device. Transactions of the CSAM, 2017; 48(12): 48–57. (in Chinese)

[23] National Technical Committee for the Standardisation of Agricultural Machinery. Test method for single grain (precision) planter: GB/6973-2005. Beijing: China Standard Press. 2006. (in Chinese)